Earth and Planetary Science Letters 388 (2014) 175–186

Contents lists available at ScienceDirect

Earth and Planetary Science Letters

www.elsevier.com/locate/epsl

Water content of the Tanzanian lithosphere from magnetotelluric data: Implications for cratonic growth and stability

Kate Selway *, Jun Yi, Shun-Ichiro Karato

Department of Geology and Geophysics, Yale University, New Haven, CT 06520, USA

ARTICLE INFO

Article history:
Received 14 May 2013
Received in revised form 3 October 2013
Accepted 12 November 2013
Available online xxxx
Editor: L. Stixrude

Keywords:
magnetotellurics
hydrogen
water
craton
lithosphere

ABSTRACT

Hydrogen strongly influences mantle rheology and is therefore an important factor in the growth and stability of cratons. Hydrogen also strongly affects electrical conductivity so it is possible to infer the hydrogen content of the lithospheric mantle in-situ and test models of craton formation using magnetotelluric data. Tanzania is an ideal natural laboratory to test hypotheses on lithospheric hydrogen content since it contains regions with very different tectonic regimes including the stable Tanzanian Craton and the East Africa Rift that is reworking lithosphere previously deformed in the East African Orogeny. Additionally, the lithosphere is well sampled by voluminous xenoliths that constrain lithospheric composition and the geotherm, which also affect electrical conductivity. Hydrogen contents were calculated for two locations in Tanzania: the first in the stable central Tanzanian Craton and the second on the eastern margin of the craton where incipient rifting is occurring. The central Tanzanian Craton was found to have a high lithospheric mantle water content of $\sim 10^{-2}$ wt% which is comparable to that of the oceanic asthenosphere and is hard to reconcile with the long-term survival of the craton. It is possible that the water was introduced into the lithosphere recently by kimberlite volcanism or that, if the lithosphere has had a high water content throughout its history, the central craton has been shielded from deformation by weaker orogens that surround it. The eastern margin of the craton has a water content of 10^{-3} to 10^{-4} wt% throughout much of the lithospheric mantle that decreases to 10^{-4} to 10^{-5} wt% at the base of the lithosphere and at depths corresponding to the uppermost plume head. Xenolith data show evidence for partial melting of the plume head and the base of the lithosphere in this dehydrated region. The partial melting and dehydration of a plume head beneath a craton is a present-day observation of the processes that may have formed cratonic roots.

1. Introduction

In order for the sub-continental lithospheric mantle (SCLM) to survive entrainment by the convecting asthenosphere it is generally believed it must be chemically depleted, making it buoyant, and dehydrated, making it viscous (Jordan, 1988; Karato and Jung, 2003; Lee et al., 2011; Lenardic and Moresi, 1999; Li et al., 2008; Mei and Kohlstedt, 2000; O'Neill et al., 2008; Pollack, 1986; Sleep et al., 2002). During partial melting of the SCLM incompatible elements such as Fe, Al, Ca and H preferentially partition into melt which ascends to form the crust, leaving the SCLM chemically depleted and dehydrated (Carlson et al., 2005; Griffin et al., 2003, 2009; Lee et al., 2011). In general the level of SCLM depletion will increase with age as the lithosphere experiences more partial melting events (Griffin et al., 2003). Therefore, it is reasonable to expect that the SCLM would be less hydrous than the asthenosphere, which has an estimated water (hydrogen) content of ~0.01 wt% (Dai and Karato, 2009; Hirschmann, 2010; Karato, 2006). However, recent evidence from xenoliths (Li et al., 2008; Peslier, 2010; Peslier et al., 2010) and magnetotellurics (MT) (Fullea et al., 2011) has suggested that some cratonic SCLM may contain hydrogen at levels similar to the asthenosphere. This is hard to reconcile with both the chemically depleted nature of the lithosphere and the fact that cratons are stable for billions of years.

The main focus of this study is to obtain insight into SCLM hydrogen distribution because it has a large influence on rheology and hence on the stability and evolution of cratons. We use a forward modeling approach in which we test models against MT observations in Tanzania. MT measures electrical conductivity, which is strongly dependent on hydrogen content in the mantle (Karato, 1990, 2006; Karato and Wang, 2013; Yoshino et al., 2009). Tanzania is an ideal natural laboratory to test hypotheses on lithospheric hydrogen content since the rheology of the Tanzanian Craton, which has remained relatively stable since c. 2.6 Ga, contrasts strongly with the surrounding lithosphere which has been multiply reworked by several major tectonothermal events (Ebinger and Sleep, 1998; Maboko, 2000; Stern, 1994;

* Corresponding author. Now at Lamont-Doherty Earth Observatory, Columbia University, Palisades, NY 10964, USA.
E-mail address: kselway@ldeo.columbia.edu (K. Selway).

0012-821X/$ – see front matter
http://dx.doi.org/10.1016/j.epsl.2013.11.024

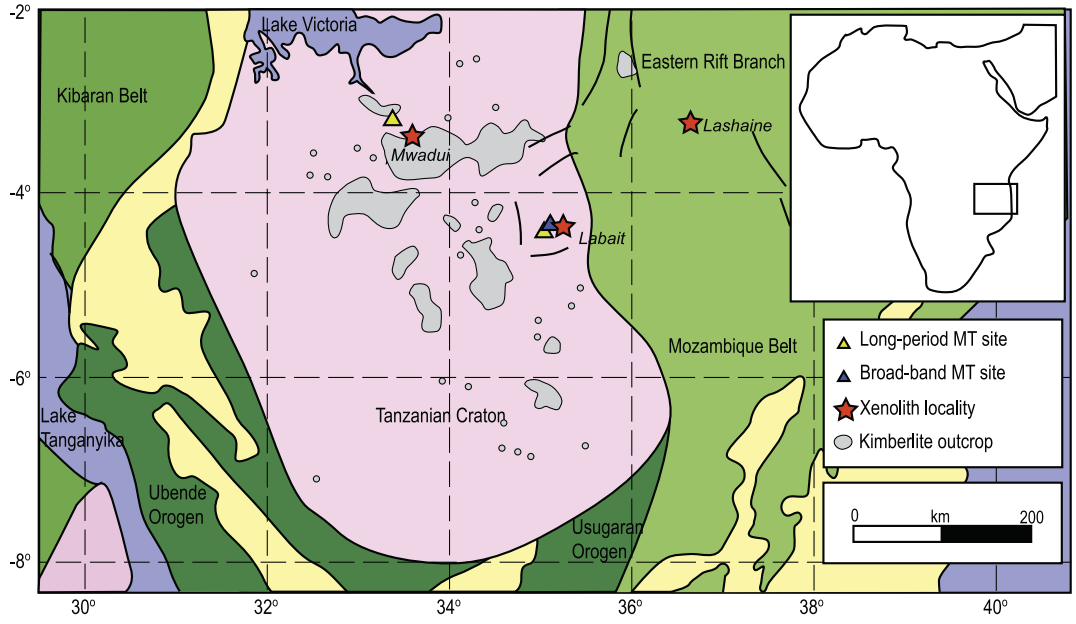

Fig. 1. Map of the study area showing the Tanzanian Craton, Usagaran Orogen, Mozambique Belt and main fault zones associated with the East African Rift. Stars show the locations of xenolith-bearing kimberlites or volcanoes that were used in this study. Triangles show the locations of MT stations used in this study, in the central Tanzanian Craton and at Labait respectively. Kimberlite localities are taken from the World Kimberlites Database (Faure, 2006).

Tenczer et al., 2007). Additionally, the Tanzanian lithosphere is well sampled by xenoliths (Bellucci et al., 2010; Chesley et al., 1999; Gibson et al., 2013; Griffin et al., 1993; Lee and Rudnick, 1999; Rudnick et al., 1994) which constrain the SCLM composition and geotherm. Constraining these variables allows the MT data to be used to determine hydrogen content (e.g. Hirth et al., 2000). We present MT data from two regions in Tanzania, one in the central Tanzanian Craton that shows no evidence for recent tectonism and one on the eastern margin of the craton that is currently undergoing incipient rifting. Together with geotherm calculations and experimentally-based predictions of electrical conductivity, we use these MT data to determine the hydrogen content of the lithospheric and upper asthenospheric mantle.

2. Geological background

The Tanzanian Craton (Fig. 1) is comprised of several Archean rock packages which cratonized by c. 2.6 Ga (Maboko, 2000; Manya et al., 2006) and have U–Pb zircon ages between ~3.0 and 2.6 Ga (Maboko, 2000; Manya et al., 2006; Möller et al., 1998). Lithospheric thickness of the Tanzanian Craton is estimated at 170–200 km from xenolith data (Griffin et al., 1993) and variably 150±20 km to 200 km (Adams et al., 2012; O'Donnell et al., 2013; Weeraratne et al., 2003) to up to 350 km (Ritsema et al., 1998) from seismic data. The Tanzanian Craton has remained stable since c. 2.6 Ga but the surrounding lithosphere has been affected by several major tectonothermal events (Fig. 1). The c. 1.8 to 2.0 Ga Usagaran Orogeny on the south-eastern side of the craton was a likely subduction-related event (Möller et al., 1995) that appears to have involved collision of a previously rifted ribbon of the Tanzanian Craton (Reddy et al., 2003). The Neoproterozoic East African Orogen (Stern, 1994) stretches several thousand kilometers through north–east Africa and Arabia, East Africa, Madagascar, India and Antarctica and was a principal collision zone in the assembly of Gondwana. In Tanzania it is represented by the c. 640 Ma north–south striking Mozambique Belt on the eastern side of the Tanzanian Craton (Stern, 1994; Tenczer et al., 2007). The orogeny reworked the Tanzanian Craton as well as introducing juvenile material (Möller et al., 1998). Since the Eocene/Late Oligocene the East African Rift System has developed along the eastern margin of Africa. Beginning with volcanism in Ethiopia at c. 40–45 Ma (Ebinger et al., 1993), rifting has progressed southwards with time. The rift bifurcates around the Tanzanian Craton with most magmatism in this region having occurred within the last 12 Myr (Corti et al., 2007; Roberts et al., 2012). Gravity (Ebinger et al., 1989; Moucha and Forte, 2011), petrological (Aulbach et al., 2008; Hilton et al., 2011; Pik et al., 2006) and seismic data (Adams et al., 2012; Fishwick and Bastow, 2011; Prodehl et al., 1997; Ritsema and van Heijst, 2000; Weeraratne et al., 2003) suggest that one or more mantle plumes are responsible for the East African Rift. The Tanzanian Craton sits at an average elevation of 1250 m due to the thermal impact of the plume (Ebinger et al., 1989).

The long history of deformation surrounding the Tanzanian Craton suggests that the craton is significantly stronger than the surrounding lithosphere and makes it an ideal place to test models for lithospheric hydrogen content. Two locations will be analyzed in this work (Fig. 1). The first is in the central Tanzanian Craton, ~80 km south–east of Mwanza. This region is considered 'pristine' cratonic lithosphere, although it is likely to be underlain by a plume head (Weeraratne et al., 2003). Additionally, xenoliths from the c. 40 to 53 Ma Mwadui kimberlite pipe (Griffin et al., 1993; Stachel et al., 1998), located ~45 km to the south–east, allow some constraints to be made on lithospheric composition. The second location is ~5 km south of Mt Hanang on the eastern margin of the Tanzanian Craton. This region was chosen because xenoliths from nearby Labait show that asthenospheric melts from the plume have refertilized the lowermost lithosphere (Chesley et al., 1999; Lee and Rudnick, 1999; Vauchez et al., 2005) while the overlying lithosphere retains a cratonic signature. Comparison between these two locations allows an assessment of whether cratonic lithosphere is dehydrated, whether more hydrous lithosphere is more likely to be deformed and the impact of partial melting on hydrogen content.

3. Methodology

The hydrogen content of mantle xenoliths is the most direct observation of lithospheric hydrogen (e.g. Bell and Rossman, 1992;

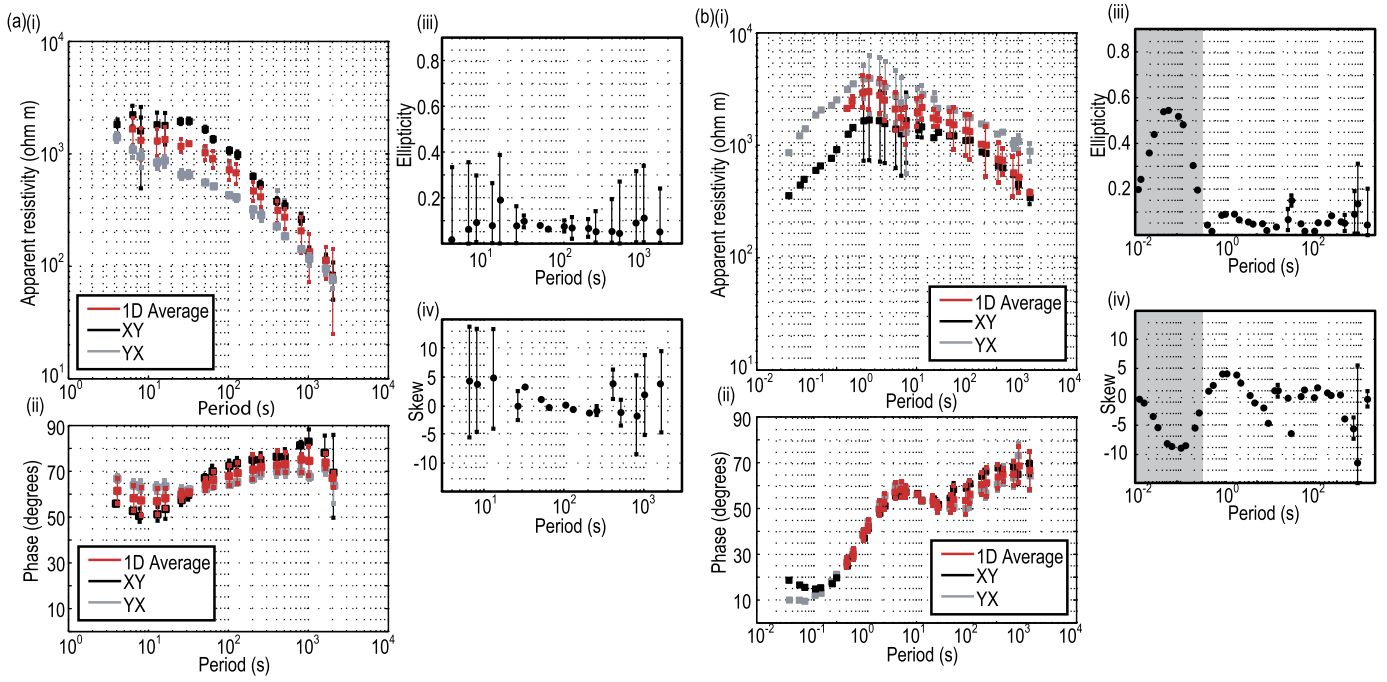

Fig. 2. MT data from (a) the central Tanzanian Craton and (b) the eastern margin of the Tanzanian Craon at Labait. (a(i)) and (b(i)) show *xy*, *yx* and the log average of apparent resistivity data, adjusted for static shift. (a(ii)) and (b(ii)) show *xy*, *yx* and the arithmetic average of phase data. Errors on the average phase data were increased to account for the difference between the *xy* and *yx* phases for each period to account for departures from true one-dimensionality. (a(iii)) and (b(iii)) show the phase tensor ellipticity, which should be below approximately 0.1 to indicate one-dimensionality and (a(iv)) and (b(iv)) show the phase tensor skew, which should be close to zero if the data are not three-dimensional. Data at Labait for periods shorter than 0.3 s have large skews and large ellipticities and were therefore not included in further analysis (grey shaded region on b(iii) and b(iv)).

Peslier et al., 2010). However, because hydrogen is highly mobile, the relationship of these observations to upper mantle hydrogen content is unclear (e.g. Demouchy and Mackwell, 2006; Gaetani et al., 2012; Mackwell and Kohlstedt, 1990; Peslier et al., 2010) and measuring hydrogen content in situ with MT may be more reliable (Fullea et al., 2011; Hirth et al., 2000; Karato, 2011). SCLM electrical resistivity is dominantly controlled by temperature and hydrogen content, with modal mineralogy and major element chemistry being less important parameters (for a review see Karato and Wang, 2013). The abundant xenoliths in the study region allow composition and temperature to be constrained so that MT data can be combined with mineral physics data to determine mantle hydrogen content.

3.1. MT data

Magnetotellurics is a passive electromagnetic geophysical method that relies on the fact that the Earth's magnetic field, which is time varying due to electrical storms and the interaction of the solar wind with the ionosphere, induces currents in conductive bodies within the Earth. Magnetic (B) and electric (E) fields are measured in orthogonal (x and y) directions at the Earth's surface as a function of time and are then transformed into the frequency domain, giving a frequency dependent impedance, Z.

$$Z_{xy} = E_x / B_y \tag{1}$$

From the impedance, the apparent resistivity (ρ_a), which is the resistivity of an equivalent uniform half-space, and the phase (ϕ), which is the offset between the electric and magnetic fields, can be determined for each angular frequency ω.

$$\rho_a = \frac{\mu_0}{\omega} |Z|^2 \tag{2}$$

$$\varphi = \arg(Z) \tag{3}$$

where μ_0 is the magnetic permeability of free space (e.g. Dmitriev and Berdichevsky, 1979).

MT data used in this project were a subset from a survey carried out in late 2011. The central Tanzanian Craton station is a long-period station with a sampling rate of 1 Hz. The Labait station was compiled from a long-period station sampled at 1 Hz and a nearby broadband station sampled at 1000 Hz. Due to the diffusive nature of EM fields, long-period stations image deeper into the mantle and broadband stations provide better crustal resolution. Data were processed using the Bounded Influence Remote Reference Processing code (Chave and Johnson, 2004). Remote referencing was implemented for the long-period stations but due to limited equipment this was not possible for broadband stations. Data quality was fair, although low source field activity limited the amount of highly coherent data at periods longer than 2000 s. Reliable responses for the Tanzanian Craton station were obtained for periods of 4 s to 2048 s. For Labait, responses from 10 s to 1428 s were taken from the long-period station and responses from 3 Hz to 10 s from the broadband station. Since the broadband station was not remote referenced, large error allowances were made for the apparent resistivity data but the phase data match well with the long-period station.

The electrical dimensionality of the data (that is, the number of directions in which the electrical resistivity of the subsurface varies) was assessed using phase tensors (Bibby et al., 2005; Caldwell et al., 2004; Thiel, 2008). The Tanzanian Craton and Labait stations were selected because they image a subsurface that is close to one-dimensional (i.e. horizontally layered), with small phase tensor skews and ellipticities generally less than 0.1 (Fig. 2), so that lateral variations in resistivity do not complicate interpretations. One-dimensional averages were calculated using an arithmetic mean for phases and log average for apparent resistivities. Since the data are not perfectly one-dimensional, errors in the one-dimensional average phase were increased to reflect the difference between the *xy* and *yx* phases to avoid fitting the data to

Table 1
Compositional depth ranges for the central Tanzanian Craton and eastern Tanzanian Craton at Labait used in electrical resistivity predictions.

Depth	Olivine	Orthopyroxene	Whole rock
Central Tanzanian Craton:			
40–110 km	88.4%, Mg#93	9.4%, Mg#93.5	Mg#92.9
110–150 km	81%, Mg#90	12.8%, Mg#92	Mg#90.3
150–200 km	77.3%, Mg#92	14.5%, Mg#92.5	Mg#91.8
Labait:			
40–70 km	76%, Mg#92	20%, Mg#92.8	Mg#92
70–110 km	79%, Mg#92.5	19%, Mg#93	Mg#92
110–150 km	73%, Mg#91	18%, Mg#92	Mg#91

a level they cannot justify. Errors in the one-dimensional apparent resistivity average were calculated from the increased phase errors (Fig. 2) (Chave and Lezaeta, 2007).

3.2. Lithospheric composition

Modal mineralogy can affect mantle resistivity although it is likely to have a much smaller effect than hydrogen content (e.g. Karato and Wang, 2013). It is therefore important to constrain both the mantle modal mineralogy and the expected level of lithospheric fertilization which is likely to correspond to hydrogen content. The Labait volcano, on the eastern margin of the Tanzanian Craton, has brought up voluminous mantle xenoliths (e.g. Aulbach et al., 2008; Chesley et al., 1999; Koornneef et al., 2009; Lee and Rudnick, 1999; Vauchez et al., 2005). Xenolith compositional data for Labait lithosphere (Table 1) are taken from Lee and Rudnick (1999). The depth to the top of the asthenospheric adiabat is ~150 km. Xenoliths from above this depth are refractory with Mg# generally between 90 and 92 (Mg# = Mg/(Mg + Fe)). At depths greater than ~130 km the lithosphere has been chemically and thermally modified, probably due to interaction with plume-related asthenospheric fluids. This region is approximately 150 °C hotter than would be expected from the shallower geotherm and some samples have experienced iron enrichment (Lee and Rudnick, 1999). Re–Os data from samples of refractory harzburgites from 80–140 km depth give Re depletion ages of 2.4 to 2.8 Ga, while those from more fertile harzburgites from 140–150 km depth give Re depletion ages of 1 Ga to the future, suggesting that the deeper lithospheric mantle has either been mixed with upwelling asthenospheric mantle or has experienced melt removal since 1 Ga (Chesley et al., 1999). Electron backscatter diffraction (EBSD), petrographic and seismic anisotropy studies (Vauchez et al., 2005) also show a progressive impact of the plume with depth. Samples from the spinel-peridotite domain (<70 km deep) are porphyroclastic and show no evidence of rift interaction while deeper samples display evidence of recent heating leading to grain-boundary mobility and nucleation recrystallization (Vauchez et al., 2005).

Xenolith data for the central Tanzanian Craton (Dawson, 1994; Griffin et al., 1993; Stachel et al., 1998) are less voluminous. Combined with data from other studies, Mwadui xenolith data suggest a depleted, harzburgitic composition at depths above ~110 km, a less depleted, lherzolitic-harzburgite composition at ~110 to ~150 km and an enriched, metasomatized lherzolitic composition at depths >150 km (Griffin et al., 1993). Proportions of olivine and orthopyroxene in harzburgite and lherzolite were taken from Griffin et al. (2009) to calculate appropriate mineral proportions for these compositions (Table 1). The thickness of the Tanzanian lithosphere was estimated to be 170 km from a combination of xenolith and seismic data (Fishwick, 2010; Griffin et al., 1993; Ritsema et al., 1998; Weeraratne et al., 2003).

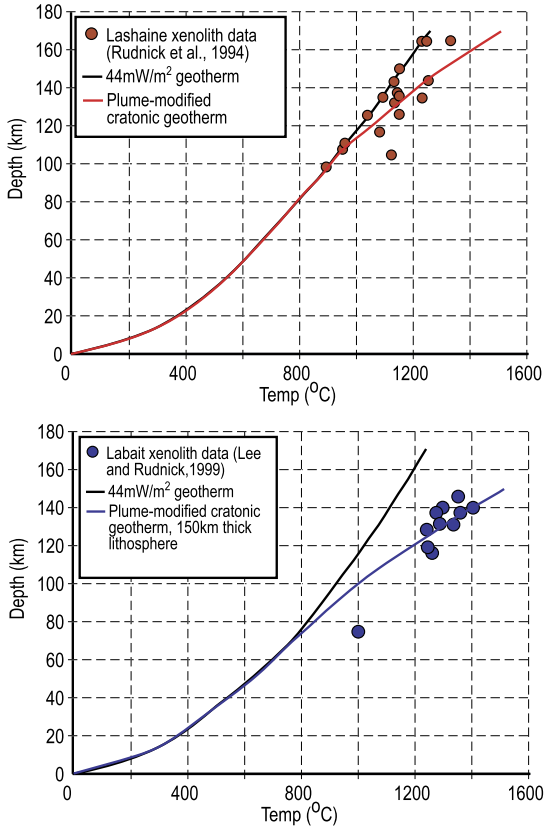

Fig. 3. Geotherm calculations in comparison with (a) Lashaine and (b) Labait xenolith thermobarometry from Rudnick et al. (1994) and Lee and Rudnick (1999). A 44 mW/m^2 cratonic geotherm fits the low-temperature Lashaine data well but does not fit the high-temperature Lashaine data or any of the Labait data, which have been reset by the mantle plume's thermal anomaly. Geotherms calculated by assuming that an initial 44 mW/m^2 cratonic geotherm has been impinged upon by a plume for ~35 Myr fit the high-temperature Lashaine xenolith data and most of the Labait data well.

3.3. Calculation of Tanzanian geotherm

Electrical conductivity is strongly influenced by temperature so it is important to accurately determine the geotherm for the two regions of interest, both in the central Tanzanian Craton and at Labait. Since the Tanzanian lithosphere is being impinged upon by a plume, the geotherm calculation must involve calculation of the initial, stable geotherm and the subsequent thermal impact of the plume. Xenolith thermobarometry can constrain both the initial and current geotherms, depending on the time at which xenoliths were thermally reset. Unfortunately, thermobarometric data are not available for Mwadui xenoliths in the central craton but xenoliths from the Lashaine volcano in north–west Tanzania (Fig. 1) show both a low-temperature, 170 km thick, ~44 mW/m^2 geotherm and a high-temperature, ~50 mW/m^2 geotherm, which are interpreted to correspond to the initial and plume-modified geotherms respectively (Rudnick et al., 1994). Lashaine xenoliths are therefore used as a proxy for the central craton. Surface heat flow values (Nyblade, 1997; Nyblade et al., 1990) can be used to determine the initial geotherm since the thermal signal from a plume that arrived at c. 40 Ma will not yet have reached the surface (Jaupart and Mareschal, 2007; Sleep et al., 2002).

We calculated the original, stable geotherms from surface heat flows and estimates of average mantle heat flows (Jaupart and Mareschal, 2007). The results agree well with Lashaine low-geotherm xenolith data (Fig. 3) (Rudnick et al., 1994). We then calculated the current, plume-affected geotherm by solving the diffusion equation for a plume that is 140 °C hotter than ambient

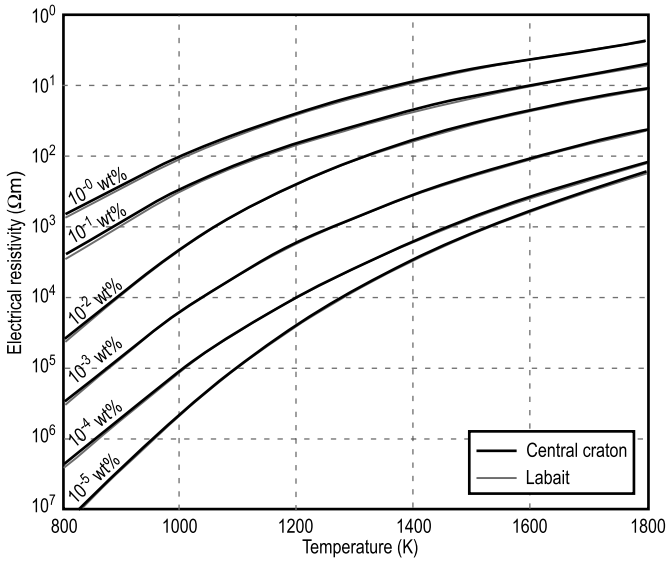

Fig. 4. Electrical resistivities for water contents between 10^{-5} wt% and 10^{0} wt% calculated for the compositions of the central Tanzanian Craton site (black) and the Labait site on the eastern edge of the Tanzanian Craton (grey).

mantle, a temperature taken from mantle potential temperatures of rift magmas (Rooney et al., 2012), seismic attenuation data (Venkataraman et al., 2004) and xenolith thermobarometry (Lee and Rudnick, 1999). Since the exact time of plume impact in Tanzania is not known, we calculated the diffusion profile for plume impact between 40 Ma (the onset of magmatism in Ethiopia), and 30 Ma, allowing uplift in Tanzania to begin at 25 Ma (Roberts et al., 2012). Differences in the resulting geotherms are negligible and a 35 Ma plume arrival, as suggested by Ebinger and Sleep (1998), was used in further calculations. For both the central Tanzanian Craton and Labait the plume-modified geotherm produces a good match to the high-temperature xenolith geotherms (Fig. 3). However, in both regions there are some xenoliths which record temperatures higher than those estimated by the plume-modified geotherm, including one mid-lithospheric sample in each region >100 °C higher than predicted. A diffusive heat flux producing such conditions would require unreasonably large lithospheric thermal conductivities and would have produced higher Moho temperatures than those measured for the region (Bellucci et al., 2011; Blondes et al., 2010). If the thermobarometric analyses are correct, these high temperatures are therefore likely to have been produced by advective heat flux through the movement of magma. Within the asthenosphere, a standard adiabatic temperature increase of 0.3 K/km (Turcotte and Schubert, 2002) was assumed beneath the central Tanzanian Craton. Beneath Labait, the mantle potential temperature of 1440 °C (Rooney et al., 2012) was used to calculate asthenospheric temperatures (McKenzie and Bickle, 1988), producing an adiabatic gradient of ∼0.7 K/km, similar to the central craton. Full details of the calculations are shown in the supplementary information.

3.4. Calculation of relationship between water content and resistivity

Resistivity was calculated assuming an olivine/orthopyroxene mixture since no other mineral fraction exists in sufficient quantities to form an interconnected pathway (Table 1). A salient feature of our modeling is to include the influence of hydrogen partitioning between olivine and orthopyroxene. Hydrogen strongly affects electrical conductivity in these minerals but hydrogen partitioning between them changes by more than an order of magnitude as a function of temperature, pressure and water fugacity (Dai and Karato, 2009). Hydrogen partitioning was calculated by comparing water solubility in olivine and orthopyroxene according to experimental results by Mierdel et al. (2007) and Kohlstedt et al. (1996). A full description of the method is given in the supplementary information. Electrical conductivity predictions were made using the effective media model to describe the behavior of the mineral mixture (McLachlan, 1987) and experimental data summarized in Karato and Wang (2013), which have been shown to be consistent with expected asthenospheric water contents (Dai and Karato, 2009). The resultant temperature-dependent electrical conductivity for the compositions of both regions at total water contents ranging from 10^{-5} wt% to 10^{0} wt% are shown in Fig. 4. The predictions are almost identical, showing that the range in modelled compositions has a negligible effect on conductivity. The maximum uncertainty in estimated water content from uncertainties in the geotherm (±100 °C) is larger than uncertainties in composition at ∼50% but is still much smaller than the range of possible water contents being investigated.

4. Results

Hypothetical lithospheres with various hydrogen contents were forward modeled and compared with the MT data, seeking the simplest hydrogen distribution that matches the data. This approach was taken since none of the available constraints are sufficiently accurate or precise to perform an inversion to calculate the hydrogen content of the lithosphere from the MT data. Since the crust may be compositionally heterogeneous and contain various conductive species, no attempt was made to analyze crustal conductivity in terms of hydrogen content. One-dimensional modeling was carried out using a Marquardt algorithm written by P. Wannamaker following the method of Petrick et al. (1977) that uses the recursive layered earth relations in Ward and Hohmann (1988). The apparent resistivity data are affected by static shifting, with the result that it is impossible to know the absolute value of the apparent resistivities. Therefore the phase data, which are unaffected by static shifting, were tested with the forward models.

4.1. Hydrogen content of the central Tanzanian Craton lithospheric mantle

The water content of the asthenosphere is generally considered to be approximately 10^{-2} wt% (Dai and Karato, 2009; Hirschmann, 2006; Karato, 2006) so forward models were initially run with resistivities in the lithospheric mantle corresponding to hydrogen contents between 10^{-2} wt% and 10^{-4} wt% and resistivities in the asthenospheric mantle corresponding to a fixed hydrogen content of 10^{-2} wt%. Since there are no broadband MT data for the central Tanzanian Craton the crustal conductivity structure cannot be accurately resolved and results from a one-dimensional inversion were used in forward modeling. The station phase data are not well reproduced by these initial models (Fig. 5a). At shorter periods, the station data have higher phases than the forward modelled data, suggesting that the conductivity of the region increases with depth more sharply than the models at these periods. Further tests showed that the station data are best matched when the conductivity to a depth of ∼90 km is higher than that predicted for a hydrogen content of 10^{-2} wt% (Fig. 5b). The modal mineralogy for this region is constrained by very few xenolith samples from nearby kimberlite pipes which have broad depth estimates but even a pure orthopyroxene composition would not produce the observed uppermost mantle conductivity (Dai and Karato, 2009). The geotherm is also is also unconstrained by xenoliths at this location but the temperature at the top of the mantle would need to be >120 °C higher than modeled to account for the observed conductivity, which is inconsistent with the very low surface heat

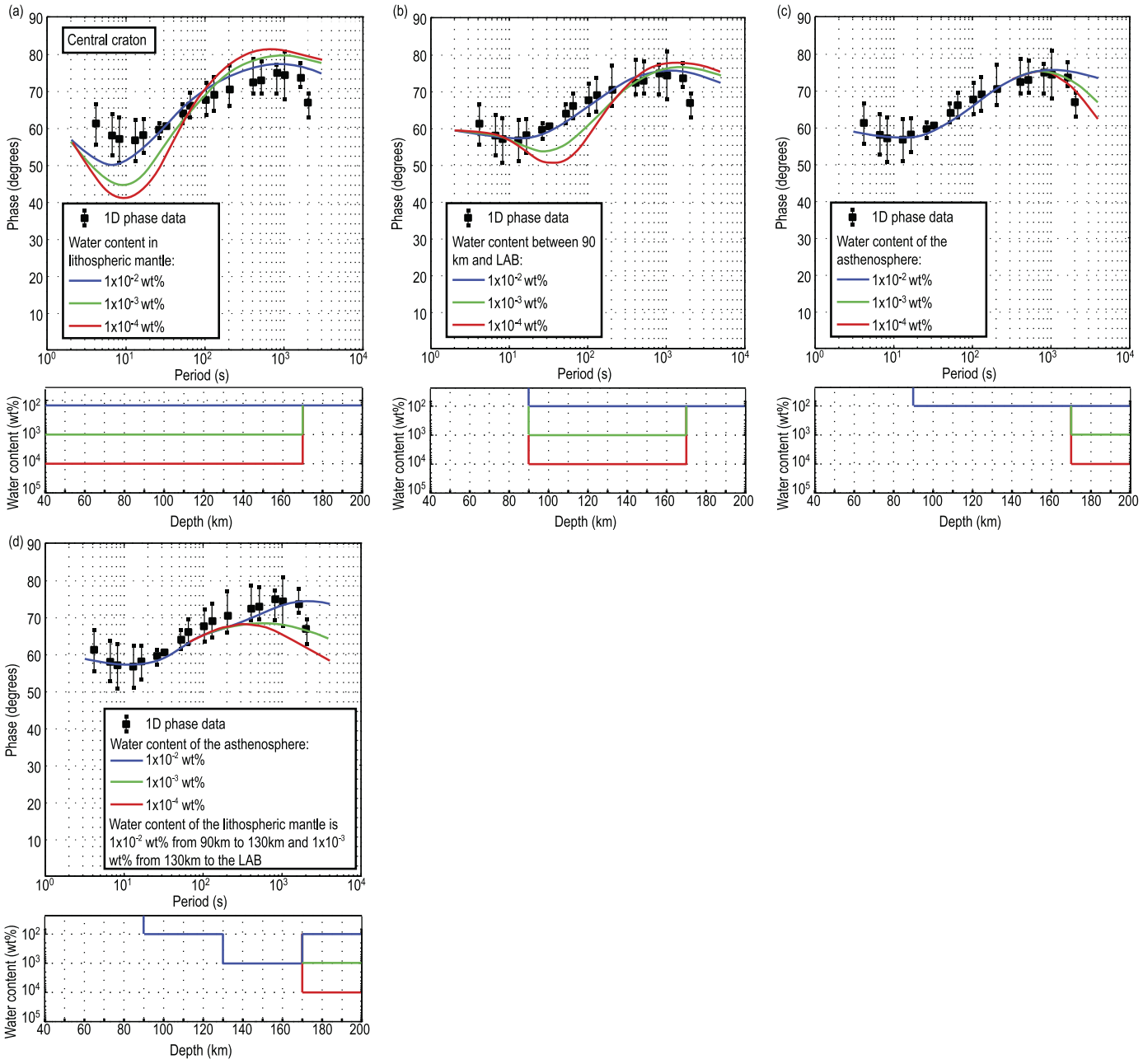

Fig. 5. Comparison between forward models and data for the central Tanzanian Craton. (a) Lithospheric mantle with water contents of 10^{-2} wt%, 10^{-3} wt% and 10^{-4} wt% and asthenosphere with water content of 10^{-2} wt%. (b) Uppermost lithospheric mantle to a depth of 90 km has a fixed conductivity corresponding to a higher hydrogen content than is feasible for the current model. From 90 km depth to the LAB at 170 km depth, the lithospheric mantle was modelled with water contents of 10^{-2} wt%, 10^{-3} wt% and 10^{-4} wt% and the asthenosphere was modelled with a fixed water content of 10^{-2} wt%. (c) The lithospheric mantle from 90 km to the LAB was modelled with a water content of 10^{-2} wt% and the asthenosphere was modelled with water contents of 10^{-2} wt%, 10^{-3} wt% and 10^{-4} wt%. (d) Test of whether a dehydrated layer might exist at the base of the lithosphere. The lithospheric mantle from 90 km to 130 km depth was modelled with a water content of 10^{-2} wt%, underlain by a 40 km thick dehydrated layer with water content 10^{-3} wt%. The asthenosphere was modelled with water contents of 10^{-2} wt%, 10^{-3} wt% and 10^{-4} wt%.

flow. Although each of these scenarios is individually unlikely, it is possible that they combine to cause the high uppermost mantle conductivity. An additional conductive species, such as grain-boundary graphite films, could also be present.

Models were run to test the hydrogen content of the lithosphere at depths >90 km (Fig. 5b). The station data are reproduced by a lithospheric conductivity structure corresponding to 10^{-2} wt% hydrogen at depths > 90 km but are not well reproduced by lower hydrogen contents. Models were also run to test the hydrogen content of the asthenosphere. The water content of the asthenosphere was varied between 10^{-2} wt% and 10^{-4} wt% while the water content below 90 km in the lithospheric mantle was fixed at 10^{-2} wt% (Fig. 5c). The longest period data point is only fit with a low asthenospheric water content of 10^{-4} wt%. Since the station data are not perfectly one-dimensional and do not extend to longer periods this result contains some ambiguity. However, phase data at the longest recorded periods from all the stations on the central Tanzanian Craton demonstrate a similar phase decrease, suggesting that the asthenosphere beneath the Tanzanian Craton may have a water content lower than the expected 10^{-2} wt%. In the Kaapvaal Craton, Peslier (2010) and Fullea et al. (2011) have proposed that the SCLM has a high hydrogen content underlain by a dehydrated lithospheric base that has allowed it to survive mantle convection. Since the SCLM hydrogen content modeled here is also high, mod-

els were run to test whether a dehydrated layer at the base of the lithosphere (40 km thick with a hydrogen content of 10^{-3} wt%) is consistent with the station data (Fig. 5d). Models with asthenospheric hydrogen contents of 10^{-2} wt% and 10^{-3} wt% fit most of the data within error but still produce a worse fit to the station data than models with no dehydrated layer. These data do not rule out the possibility that a dehydrated layer may exist at the base of the Tanzanian Craton lithosphere but certainly provide no argument that such a layer must exist.

4.2. Hydrogen content of the lithospheric mantle at Labait, on the edge of the Tanzanian Craton

Models were initially run with the SCLM hydrogen content between 10^{-2} wt% and 10^{-4} wt%, an asthenospheric hydrogen content of 10^{-2} wt% and a fixed crustal structure taken from inverse modeling of the broadband data. As for the central craton, the phase values of all forward models are smaller than the station data for periods corresponding to the uppermost mantle (Fig. 6a), showing that the uppermost mantle is more conductive than would be expected for the highest modeled water content. Further testing showed that this high conductivity layer extends to a depth of approximately 60 km and cannot be explained purely by lower crustal conductivity. This must be due to compositional and/or thermal properties following similar arguments as the central craton.

Forward models were run to test mantle hydrogen content below 60 km depth. Initial tests (Fig. 6b) were run with water contents between 60 km and 150 km varying between 10^{-2} wt% and 10^{-4} wt% and a fixed asthenospheric hydrogen content of 10^{-2} wt%. At periods less than ~50 s, water contents of 10^{-3} wt% and 10^{-4} wt% fit the data within error while the 10^{-2} wt% model does not fit the data. At longer periods, the forward modeled phases for all water contents are higher than the station phases. This suggests that at greater depths, the conductivity of the subsurface does not increase with depth as sharply as predicted by the models. Therefore, forward models were run in which the hydrogen content decreases with depth. The water content of the asthenosphere was tested by setting the asthenospheric water content at an order of magnitude less than that of the lithosphere (Fig. 6c). Water contents of 10^{-3} wt% and 10^{-4} wt% between 60 km and 150 km that decrease to 10^{-4} wt% and 10^{-5} wt% respectively in the asthenosphere fit the data well. To test whether it is possible to resolve the depth at which the water content decreases, models were run in which the water content decreases at 120 km rather than at 150 km (Fig. 6d). Visually, these models provide an even closer fit to the data but since all models fit the data to within error, the specific depth at which this water decrease occurs cannot be resolved. Finally, since the asthenosphere is expected to have a hydrogen content of 10^{-2} wt%, a test was run to determine whether the data can be fit by a dry layer at the base of the lithosphere that is underlain by a more hydrogen-rich asthenosphere. The resulting models do not fit the data (Fig. 6e) and show that these data require the asthenosphere to have a hydrogen content that is lower than 10^{-2} wt%.

5. Discussion

5.1. Hydrogen content of the central Tanzanian Craton lithospheric mantle

Forward modeling shows that the bulk of the central Tanzanian Craton SCLM in the study region contains approximately 10^{-2} wt% water, which implies that olivine is almost water-saturated. This is a surprising result given the longevity of the Tanzanian Craton and its resistance to deformation during major orogenic events. At a given pressure and temperature in the lithospheric upper mantle, a transition from dry to water-saturated conditions will be accompanied by a decrease in viscosity of more than two orders of magnitude (Karato, 2010). Geodynamic modeling shows that there must be a significant contrast in viscosity between cratonic lithosphere and underlying convecting mantle to allow cratonic lithosphere to survive (Lenardic and Moresi, 1999; O'Neill et al., 2008) and such models generally require a dry lithosphere and wet asthenosphere (e.g. O'Neill et al., 2008). The suggestion that the asthenosphere may have a low water content is not definitive because of insufficient long-period data, data quality and departures from one-dimensionality. However, even if the asthenosphere is assumed to be wet, it is not realistic for a water-saturated craton to have survived for 2 Gyr. There are several possible explanations for this:

(1) The cratonic lithosphere may be underlain by a dehydrated root.

Xenolith hydrogen contents (Baptiste et al., 2012; Peslier et al., 2010) and MT data (Fullea et al., 2011) from the Kaapvaal Craton suggest that the bulk of the SCLM has hydrogen contents up to 10^{-2} wt% but that the base of the craton is within error of being completely dry. Peslier et al. (2010) suggested that this dry base allows the craton to survive. Although we consider this possibility to be geodynamically unlikely, the tests shown in Fig. 6(d) were designed to examine whether such a dehydrated layer might exist at the base of the Tanzanian Craton SCLM. These tests were inconclusive since the best fitting model (Fig. 6c) does not contain a dehydrated lithospheric base but the improvement in this model fit relies only on one data point.

(2) The cratonic lithosphere may be surrounded by weaker mobile belts that protect it from deformation.

Geodynamic modeling shows that zones of pre-existing weakness around a craton will be preferentially deformed, protecting the craton from deformation (Lenardic et al., 2003). The Tanzanian Craton is surrounded by mobile belts and many structures have experienced several periods of reactivation (e.g. Reddy et al., 2004; Tenczer et al., 2007) including current faulting along the East Africa Rift which is strongly controlled by the location of the East African Orogen (Chorowicz, 2005). In addition, material from the Tanzanian Craton was involved in both the Usagaran Orogeny (Reddy et al., 2004) and the East African Orogeny (Sommer et al., 2005), showing that the craton as a whole has not actually survived for the last 2 Gyr. It is possible that successive orogenic events have progressively deformed and weakened the edges of the Tanzanian Craton such that subsequent deformation is preferentially partitioned into them.

(3) The water may have been recently added to the lithosphere by kimberlites.

The water content of the central Tanzanian Craton has not necessarily been high throughout its entire history; instead, the water may have been added by recent kimberlite volcanism. Measured water contents of kimberlite samples are commonly 5 wt% to 10 wt% (Francis and Patterson, 2009). Although some of this water is likely to be meteoric (Kamenetsky et al., 2007; Stripp et al., 2006) source magmas are also more hydrous than the lithosphere into which they intrude (Kopylova et al., 2007). Kimberlites interact extensively with the lithosphere (Francis and Patterson, 2009) and, since hydrogen diffuses very easily (Karato, 2006), portions of the lithosphere that interact with kimberlite melts should be hydrated. The majority of Tanzanian kimberlites have erupted within the last 80 Myr (Chesler, 2012) and the MT site location is proximal to the large, c. 40 to 53 Ma Mwadui kimberlite pipe and could therefore have been hydrated by it. The localized nature of this kimberlite-driven hydration and the recent ages of kimberlite

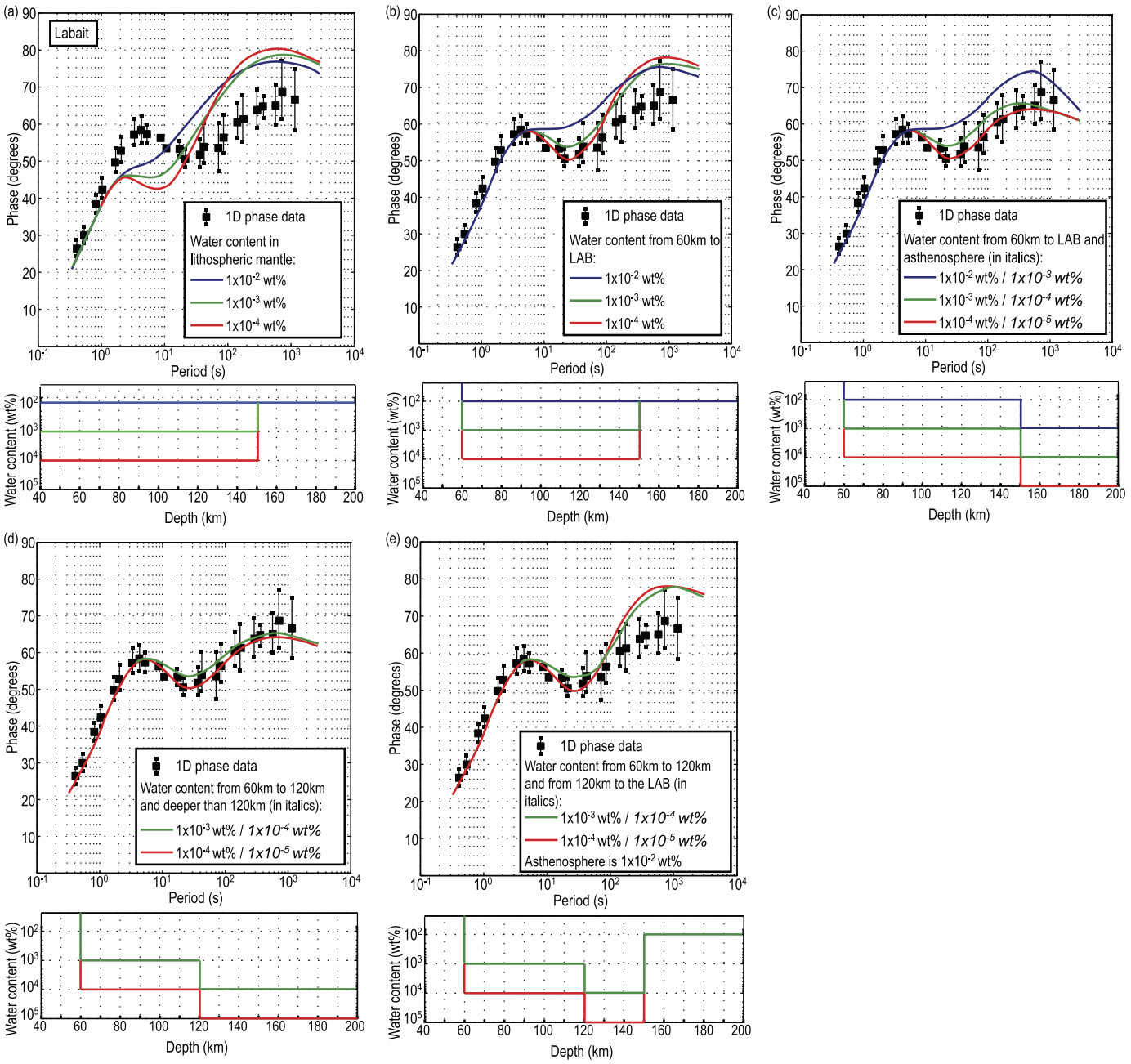

Fig. 6. Comparison between forward models and data for the Labait region on the eastern margin of the Tanzanian Craton. (a) Lithospheric mantle was modelled with water contents of 10^{-2} wt%, 10^{-3} wt% and 10^{-4} wt% and asthenosphere with water content of 10^{-2} wt%. (b) Uppermost lithospheric mantle to a depth of 60 km has a fixed conductivity corresponding to a higher hydrogen content than is feasible for the current model. From 60 km depth to the LAB at 150 km depth, the lithospheric mantle was modelled with water contents of 10^{-2} wt%, 10^{-3} wt% and 10^{-4} wt% and the asthenosphere was modelled with a fixed water content of 10^{-2} wt%. (c) Test of the effect of decreasing the water content of the asthenosphere with respect to the lithospheric mantle. Water contents are modelled decreasing from 10^{-2} wt% between 60 km and the LAB to 10^{-3} wt% in the asthenosphere, 10^{-3} wt% between 60 km and the LAB to 10^{-4} wt% in the asthenosphere and 10^{-4} wt% between 60 km and the LAB to 10^{-5} wt% in the asthenosphere. (d) Test of the effect of changing the depth at which the water content decreases from the LAB to 120 km. Water contents are modelled decreasing from 10^{-3} wt% between 60 km and the 120 km to 10^{-4} wt% at greater depths and 10^{-4} wt% between 60 km and 120 km to 10^{-5} wt% at greater depths. (e) Test of the effect of a dehydrated layer at the base of the lithosphere with a more hydrous asthenosphere. Asthenospheric water content was set at 10^{-2} wt%. Within the lithosphere, models were run with the water content decreasing from 10^{-3} wt% between 60 km and the 120 km to 10^{-4} wt% between 120 km and 150 km and from 10^{-4} wt% between 60 km and 120 km to 10^{-5} wt% between 120 km and 150 km.

intrusion remove the paradox of a hydrogen-rich lithosphere surviving for several billion years.

A similar argument could be made for the observed hydrogen-rich nature of the Kaapvaal Craton, which experienced some Proterozoic kimberlite intrusions (Donnelly et al., 2011; Phillips et al., 1989; Seggie et al., 1999) but voluminous intrusions in the Jurassic and Cretaceous (Allsopp and Barrett, 1975; Phillips et al., 1998; Smith et al., 1994). The young ages of the bulk of the kimberlite magmatism show that the craton does not need to survive with any subsequent hydration for cratonic time scales. The MT sites analyzed by Fullea et al. (2011) were located close to kimberlites and all analyzed xenoliths are also related to kimberlites. Therefore it is possible that the observed patterns are caused by kimberlite-hosted hydration of the lithosphere and are not a generic lithospheric characteristic. Indeed, Archean lithosphere of the Superior Craton, which is at least 150 km from kimberlites that we are

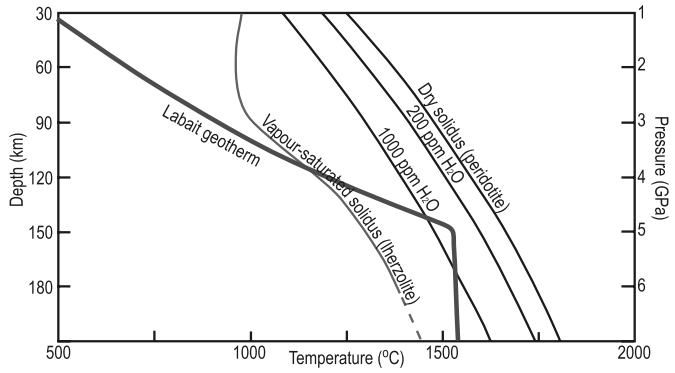

Fig. 7. The calculated geotherm at Labait (thick grey line) with the dry, 200 ppm water and 1000 ppm water peridotite solidus curves (Aubaud et al., 2004) and the vapour-saturated lherzolite solidus curve (Green et al., 2010).

aware of Armstrong et al. (2004), Moser and Heaman (1997), was found to be anhydrous, as would be expected for cratonic lithosphere (Hirth et al., 2000).

5.2. Hydrogen content of the lithospheric mantle on the edge of the Tanzanian Craton at Labait

Forward modeling shows that, beneath a region of higher conductivity to a depth of approximately 60 km, the lithosphere at Labait has a water content of 10^{-3} to 10^{-4} wt% to a depth of 120 to 150 km, below which the water content decreases to 10^{-4} to 10^{-5} wt%. The low water content throughout most of the lithosphere is typical of what would be expected for stable, cratonic lithosphere. Xenoliths from approximately 130 km depth at Labait show evidence of enrichment from interaction with asthenospheric melts and partial melting (Chesley et al., 1999; Lee and Rudnick, 1999; Vauchez et al., 2005), corresponding to the dehydrated region. Since hydrogen preferentially partitions into melt (e.g. Hirschmann et al., 2009; Hirth and Kohlstedt, 1996), the solid fraction will be dehydrated after partial melting. A comparison of the calculated Labait geotherm with phase diagrams of peridotite (Aubaud et al., 2004) and fertile lherzolite (Green et al., 2010) show that a peridotite plume with a water content of several hundred ppm or a more fertile plume with a lower water content would melt at the top of the asthenosphere at Labait (Fig. 7).

Xenoliths from many locations worldwide have sampled a fertile sheared lherzolite layer at the base of the lithosphere that is characterized by enriched incompatible element compositions and is thought to have been formed by interaction with asthenospheric melts (O'Reilly and Griffin, 2010), which bears obvious similarities to the fertile layer at the base of the lithosphere at Labait (Chesley et al., 1999; Lee and Rudnick, 1999; Vauchez et al., 2005). Since water behaves as an incompatible element, the enriched sheared lherzolites could be expected to have higher water contents than the overlying depleted lithosphere. However, as discussed above it is difficult to reconcile a weak, hydrated lithospheric base with the survival of continental SCLM. Additionally, some mineral physics data suggest that sheared lherzolites are dehydrated (Skemer and Karato, 2008). Results from Labait support the argument for dry sheared lherzolites by showing that the enriched incompatible element compositions at the base of the lithosphere are associated with a decrease in water content. This pattern of greater enrichment in incompatible elements other than water has been observed elsewhere. In studies of plume-generated ocean island basalts, Workman et al. (2006) and Dixon et al. (2002) found that enriched mantle plume sources equivalent to those in Tanzania (EM-type or HIMU-type; Aulbach et al., 2008; Bizimis et al., 2003; Paslick et al., 1995) have lower ratios of water to other incompatible elements than a common mantle source. Workman et al. (2006) suggest that this is due to the fast diffusion of hydrogen; the hydrogen content of the enriched plume source will decrease until equilibrium is reached with ambient mantle but other incompatible elements will not reach equilibrium even over time scales of the age of the Earth.

The observation that the plume material in the uppermost asthenosphere is dehydrated has important implications for theories of the formation and survival of cratons. Cratonic roots are commonly thought to nucleate and grow either by accretionary stacking of oceanic lithosphere or by subcretion of mantle plume material (Arndt et al., 2009; Aulbach, 2012; Griffin et al., 2003; Smithies et al., 2005; Wyman and Kerrich, 2002). A recent compilation of global cratonic geochemical and thermobarometric data found considerable evidence for craton nucleation from plumes with excess T_P (Aulbach, 2012). Plume dehydration has been previously observed at the central Pacific plume, which Karato (2008) argued is dehydrated compared to the surrounding asthenosphere based on seismic anisotropy, electrical resistivity and viscosity data. Analysis of MT data by Constable and Heinson (2004) suggested that, apart from a region of interconnected melt, the uppermost asthenosphere surrounding the Hawaiian plume has resistivities consistent with dehydrated olivine. The unambiguous observation of dehydrated uppermost asthenosphere beneath Labait is a present-day demonstration of the processes that may have formed cratonic roots. As the plume head partially melts it becomes dehydrated and depleted. The resulting melts are likely to metasomatize overlying lithosphere and cause it to become hydrated and refertilized. However, the depleted and dehydrated residue from the upper asthenospheric partial melting will become more viscous and chemically distinct from the surrounding asthenosphere – in effect, becoming the base of the lithosphere. Indeed, the very presence of a sheared lherzolite layer, which has formed through interaction with asthenospheric melts, may suggest that the underlying asthenosphere is at least partially dehydrated and strong and is serving to protect the lithosphere. The characteristics seen in this region suggest that where a plume impact does not completely rift continental lithosphere and create new oceanic lithosphere, it will instead lead to thickening of the continental lithosphere.

5.3. General implications for the interpretation of MT data

Lateral variations in lithospheric conductivity of several orders of magnitude are commonly observed worldwide, even in regions of tectonic stability such as central Australia (Selway et al., 2009), the Kaapvaal Craton (Evans et al., 2011), the Canadian Shield (Jones et al., 2005) and the São Francisco Craton (Bologna et al., 2011). Since small amounts of water can have a large effect on conductivity, it has seemed likely that these variations could be caused by lateral variations in water content (Selway, 2013). Tanzania is an ideal place to test this hypothesis since lithospheric composition and geotherms are well constrained. The analysis presented here shows that the Tanzanian Craton SCLM water content differs by approximately two orders of magnitude over a lateral distance of only approximately 300 km. All the possible mechanisms for introducing or removing water from the Tanzanian lithosphere are related to tectothermal events, be that through hydration via kimberlite interaction or dehydration via plume-related partial melting or high-temperature orogenic events. The hydrogen content of the SCLM preserves a record of tectonic processes, particularly enrichment events that introduce hydrogen into the lithosphere and high-temperature partial melting events that remove it. Since hydrogen has such a large effect on the electrical conductivity of lithospheric mantle, MT can therefore be used as a tool to image the record of tectonism on the lithosphere.

6. Conclusions

Combined MT, mineral physics and xenolith petrology and thermobarometric data were used to constrain the hydrogen content of the lithospheric and uppermost asthenospheric mantle at two locations in Tanzania – the first in the central Tanzanian Craton and the second on the eastern margin of the Tanzanian Craton at Labait. The region was chosen partly because the abundance of mantle xenoliths allows the composition and thermal structure of the lithosphere to be well constrained and partly because of its interesting tectonic history in which the Tanzanian Craton has survived for 2 Gyr while several major tectonic events, including the current East Africa Rift, have deformed the surrounding lithosphere.

The central Tanzanian Craton SCLM from 90 km to the LAB has a hydrogen content of approximately 10^{-2} wt%, which is the water content in typical oceanic asthenosphere. Conductivities in the shallower mantle correspond to even higher water contents for the calculated composition and geotherm. This is a surprising result since hydrogen significantly weakens the mantle and a cratonic region that has survived multiple large tectonic events is expected to be dehydrated. We propose that the hydrogen may have been introduced into the lithosphere recently by Jurassic to Cretaceous kimberlites. The SCLM beneath the eastern margin of the Tanzanian Craton at Labait has a lower water content of 10^{-3} wt% to 10^{-4} wt% from 60 km to between 120 and 150 km which decreases even further to 10^{-4} wt% to 10^{-5} wt% at greater depths corresponding to the plume head. The decrease in water content near the base of the lithosphere agrees with xenolith data that show evidence of partial melting at the base of the lithosphere and at the top of the asthenosphere, which would leave the residual mantle dehydrated. This may be a present-day expression of the processes that have formed cratonic roots in the past in which a plume head in the upper asthenospheric mantle is partially melted, causing it to become dehydrated and depleted to such a degree that it becomes the base of the lithosphere.

These results have demonstrated that hydrogen contents in SCLM can vary by two to three orders of magnitude over lateral distances of only a few hundred kilometers. We therefore suggest that variations in SCLM hydrogen contents are a likely explanation for large lateral conductivity variations observed in many locations worldwide. MT can be an important tool in determining the water content of the asthenosphere, the enrichment state of the lithosphere and therefore the geological history of regions.

Acknowledgements

This work was funded by Australian Research Council grant DP0988263 and National Science Foundation grant EAR-1069423. K.S. is grateful to COSTECH, regional and district governments and locals in Tanzania for permission to carry out field work and to the University of Dar es Salaam, M. Khalfan and G. Boren for assistance in field work. P. Wannamaker generously provided the 1D code and S. Thiel provided the phase tensor code. J.P. O'Donnell provided valuable assistance in geotherm calculations. This manuscript was improved by thoughtful and helpful reviews by C.-T. Lee and A. Nyblade.

Appendix A. Supplementary material

Supplementary material related to this article can be found online at http://dx.doi.org/10.1016/j.epsl.2013.11.024.

References

Adams, A., Nyblade, A., Weeraratne, D., 2012. Upper mantle shear wave velocity structure beneath the East African plateau: evidence for a deep, plateauwide low velocity anomaly. Geophys. J. Int. 189, 123–142.
Allsopp, H., Barrett, D., 1975. Rb–Sr age determinations on South African kimberlite pipes. Phys. Chem. Earth 9, 605–617.
Armstrong, K., Nowicki, T., Read, G., 2004. Kimberlite AT-56: a mantle sample from the north central Superior craton Canada. Lithos 77, 695–704.
Arndt, N., Coltice, N., Helmstaedt, H., Gregoire, M., 2009. Origin of Archean subcontinental lithospheric mantle: Some petrological constraints. Lithos 109, 61–71.
Aulbach, S., 2012. Craton nucleation and formation of thick lithospheric roots. Lithos 149, 16–30.
Aubaud, C., Hauri, E.H., Hirschmann, M.M., 2004. Hydrogen partition coefficients between nominally anhydrous minerals and basaltic melts. Geophys. Res. Lett. 31, L20611.
Aulbach, S., Rudnick, R.L., McDonough, W.F., 2008. Li–Sr–Nd isotope signatures of the plume and cratonic lithospheric mantle beneath the margin of the rifted Tanzanian craton (Labait). Contrib. Mineral. Petrol. 155, 79–92.
Baptiste, V., Tommasi, A., Demouchy, S., 2012. Deformation and hydration of the lithospheric mantle beneath the Kaapvaal craton South Africa. Lithos 149, 31–50.
Bell, D.R., Rossman, G.R., 1992. Water in Earth's mantle – the role of nominally anhydrous minerals. Science 255, 1391–1397.
Bellucci, J.J., McDonough, W.F., Rudnick, R.L., 2010. Thermal history and origin of the Tanzanian Craton from Pb isotope thermochronology of feldspars from lower crustal xenoliths. Geochim. Cosmochim. Acta 74, A75.
Bellucci, J.J., McDonough, W.F., Rudnick, R.L., 2011. Thermal history and origin of the Tanzanian Craton from Pb isotope thermochronology of feldspars from lower crustal xenoliths. Earth Planet. Sci. Lett. 301, 493–501.
Bibby, H.M., Caldwell, T.G., Brown, C., 2005. Determinable and non-determinable parameters of galvanic distortion in magnetotellurics. Geophys. J. Int. 163, 915–930.
Bizimis, M., Salters, V.J.M., Dawson, J.B., 2003. The brevity of carbonatite sources in the mantle: evidence from Hf isotopes. Contrib. Mineral. Petrol. 145, 281–300.
Blondes, M.S., Rudnick, R.L., Ramezani, J., Piccoli, P.M., Bowring, S.A., 2010. Slow cooling in the lowermost crust of a continent–continent collision: Evidence from accessory phase U–Pb thermochronology of deep crustal xenoliths from the Mozambique Belt Tanzania. Geochim. Cosmochim. Acta 74, A97.
Bologna, M.S., Padilha, A.L., Vitorello, Í., Pádua, M.B., 2011. Signatures of continental collisions and magmatic activity in central Brazil as indicated by a magnetotelluric profile across distinct tectonic provinces. Precambrian Res. 185, 55–64.
Caldwell, T.G., Bibby, H.M., Brown, C., 2004. The magnetotelluric phase tensor. Geophys. J. Int. 158, 457–469.
Carlson, R.W., Pearson, D.G., James, D.E., 2005. Physical, chemical, and chronological characteristics of continental mantle. Rev. Geophys. 43.
Chave, A.D., Johnson, D.J., 2004. Bounded influence magnetotelluric response function estimation. Geophys. J. Int. 157, 988–1006.
Chave, A.D., Lezaeta, P., 2007. The statistical distribution of magnetotelluric apparent resistivity and phase. Geophys. J. Int. 171, 127–132.
Chesler, R., 2012. The Geochemistry and Geochronology of Tanzanian Kimberlites. School of Earth Sciences, The University of Melbourne, Melbourne.
Chesley, J.T., Rudnick, R.L., Lee, C.T., 1999. Re–Os systematics of mantle xenoliths from the East African Rift: Age, structure, and history of the Tanzanian craton. Geochim. Cosmochim. Acta 63, 1203–1217.
Chorowicz, J., 2005. The East African rift system. J. Afr. Earth Sci. 43, 379–410.
Constable, S., Heinson, G., 2004. Hawaiian hot-spot swell structure from seafloor MT sounding. Tectonophysics 389, 111–124.
Corti, G., van Wijk, J., Cloetingh, S., Morley, C.K., 2007. Tectonic inheritance and continental rift architecture: Numerical and analogue models of the East African Rift system. Tectonics 26.
Dai, L., Karato, S.-i., 2009. Electrical conductivity of orthopyroxene: Implications for the water content of the asthenosphere. Proc. Jpn. Acad. Ser. B, Phys. Biol. Sci. 85, 466–475.
Dawson, J.B., 1994. Quaternary kimberlitic volcanism on the Tanzania Craton. Contrib. Mineral. Petrol. 116, 473–485.
Demouchy, S., Mackwell, S., 2006. Mechanisms of hydrogen incorporation and diffusion in iron-bearing olivine. Phys. Chem. Miner. 33, 347–355.
Dixon, J.E., Leist, L., Langmuir, C., Schilling, J.-G., 2002. Recycled dehydrated lithosphere observed in plume-influenced mid-ocean-ridge basalt. Nature 420, 385–389.
Dmitriev, V.I., Berdichevsky, M.N., 1979. The fundamental model of magnetotelluric sounding. Proc. IEEE 67, 1034–1044.
Donnelly, C.L., Griffin, W.L., O'Reilly, S.Y., Pearson, N.J., Shee, S.R., 2011. The kimberlites and related rocks of the Kuruman kimberlite province, Kaapvaal craton South Africa. Contrib. Mineral. Petrol. 161, 351–371.
Ebinger, C., Sleep, N., 1998. Cenozoic magmatism throughout east Africa resulting from impact of a single plume. Nature 395, 788–791.
Ebinger, C., Bechtel, T., Forsyth, D., Bowin, C., 1989. Effective elastic plate thickness beneath the East African and Afar plateaus and dynamic compensation of the uplifts. J. Geophys. Res. 94, 2883–2901.

Ebinger, C., Yemane, T., Woldegabriel, G., Aronson, J., Walter, R., 1993. Late Eocene–Recent volcanism and faulting in the southern main Ethiopian rift. J. Geol. Soc. 150, 99–108.
Evans, R.L., Jones, A.G., Garcia, X., Muller, M., Hamilton, M., Evans, S., Fourie, C., Spratt, J., Webb, S., Jelsma, H., 2011. Electrical lithosphere beneath the Kaapvaal craton, southern Africa. J. Geophys. Res. 116, B04105.
Faure, S., 2006. World kimberlites database. Version 2006-2. Consortium de Recherche en Exploration Minérale.
Fishwick, S., 2010. Surface wave tomography imaging of the lithosphere–asthenosphere boundary beneath central and southern Africa. Lithos 120, 63–73.
Fishwick, S., Bastow, I.D., 2011. Towards a better understanding of African topography: a review of passive-source seismic studies of the African crust and upper mantle. Geol. Soc. (Lond.) Spec. Publ. 357, 343–371.
Francis, D., Patterson, M., 2009. Kimberlites and aillikites as probes of the continental lithospheric mantle. Lithos 109, 72–80.
Fullea, J., Muller, M.R., Jones, A.G., 2011. Electrical conductivity of continental lithospheric mantle from integrated geophysical and petrological modeling: Application to the Kaapvaal Craton and Rehoboth Terrane, southern Africa. J. Geophys. Res., Solid Earth 116.
Gaetani, G.A., O'Leary, J.A., Shimizu, N., Bucholz, C.E., Newville, M., 2012. Rapid reequilibration of H_2O and oxygen fugacity in olivine-hosted melt inclusions. Geology 40, 915–918.
Gibson, S.A., McMahon, S.C., Day, J.A., Dawson, J.B., 2013. Highly refractory lithospheric mantle beneath the Tanzanian Craton: Evidence from Lashaine Pre-metasomatic Garnet-bearing peridotites. J. Petrol. 54, 1503–1546.
Green, D.H., Hibberson, W.O., Kovács, I., Rosenthal, A., 2010. Water and its influence on the lithosphere–asthenosphere boundary. Nature 467, 448–451.
Griffin, W., O'Reilly, S., Abe, N., Aulbach, S., Davies, R., Pearson, N., Doyle, B., Kivi, K., 2003. The origin and evolution of Archean lithospheric mantle. Precambrian Res. 127, 19–41.
Griffin, W.L., Ryan, C., O'Reilly, S.Y., Nixon, P., Win, T., 1993. Trace elements in garnets from Tanzanian kimberlites: Relation to diamond content and tectonic setting. In: Meyer, H.O.A., Leonardos, O.H. (Eds.), Proceedings of the Fifth International Kimberlite Conference. Comp. de Pesquisa de Recursos Miner., Arax, Brazil, pp. 145–147.
Griffin, W.L., O'Reilly, S.Y., Afonso, J.C., Begg, G.C., 2009. The composition and evolution of lithospheric mantle: a re-evaluation and its tectonic implications. J. Petrol. 50, 1185–1204.
Hilton, D., Halldórsson, S., Barry, P., Fischer, T., de Moor, J., Ramirez, C., Mangasini, F., Scarsi, P., 2011. Helium isotopes at Rungwe Volcanic Province, Tanzania, and the origin of East African Plateaux. Geophys. Res. Lett. 38, L21304.
Hirschmann, M.M., 2006. Water, melting, and the deep Earth H_2O cycle. Annu. Rev. Earth Planet. Sci. 34, 629–653.
Hirschmann, M.M., 2010. Partial melt in the oceanic low velocity zone. Phys. Earth Planet. Inter. 179, 60–71.
Hirschmann, M.M., Tenner, T., Aubaud, C., Withers, A., 2009. Dehydration melting of nominally anhydrous mantle: The primacy of partitioning. Phys. Earth Planet. Inter. 176, 54–68.
Hirth, G., Kohlstedt, D.L., 1996. Water in the oceanic upper mantle: implications for rheology, melt extraction and the evolution of the lithosphere. Earth Planet. Sci. Lett. 144, 93–108.
Hirth, G., Evans, R.L., Chave, A.D., 2000. Comparison of continental and oceanic mantle electrical conductivity: Is the Archean lithosphere dry. Geochem. Geophys. Geosyst. 1, 1030.
Jaupart, C., Mareschal, J., 2007. Heat flow and thermal structure of the lithosphere. Treatise on Geophysics, vol. 6, pp. 217–251.
Jones, A.G., Ledo, J., Ferguson, I.J., Farquharson, C., Garcia, X., Grant, N., McNeice, G., Roberts, B., Spratt, J., Wennberg, G., 2005. The electrical resistivity structure of Archean to Tertiary lithosphere along 3200 km of SNORCLE profiles, northwestern Canada. Can. J. Earth Sci. 42, 1257–1275.
Jordan, T.H., 1988. Structure and formation of the continental tectosphere. J. Petrol., 11–37.
Kamenetsky, V.S., Kamenetsky, M.B., Sharygin, V.V., Faure, K., Golovin, A.V., 2007. Chloride and carbonate immiscible liquids at the closure of the kimberlite magma evolution (Udachnaya-East kimberlite, Siberia). Chem. Geol. 237, 384–400.
Karato, S., 1990. The role of hydrogen in the electrical-conductivity of the upper mantle. Nature 347, 272–273.
Karato, S., 2006. Remote sensing of hydrogen in Earth's mantle. In: Keppler, H.S.J.R. (Ed.), Water in Nominally Anhydrous Minerals, pp. 343–375.
Karato, S.-i., 2008. Insights into the nature of plume–asthenosphere interaction from central Pacific geophysical anomalies. Earth Planet. Sci. Lett. 274, 234–240.
Karato, S., 2010. Rheology of the deep upper mantle and its implications for the preservation of the continental roots: A review. Tectonophysics 481, 82–98.
Karato, S.-i., 2011. Water distribution across the mantle transition zone and its implications for global material circulation. Earth Planet. Sci. Lett. 301, 413–423.
Karato, S.I., Jung, H., 2003. Effects of pressure on high-temperature dislocation creep in olivine. Philos. Mag. 83, 401–414.
Karato, S., Wang, D., 2013. Electrical conductivity of minerals and rocks. In: Karato, S. (Ed.), Physics and Chemistry of the Deep Earth. Wiley-Blackwell, New York, pp. 145–182.
Kohlstedt, D., Keppler, H., Rubie, D., 1996. Solubility of water in the α, β and γ phases of $(Mg,Fe)_2SiO_4$. Contrib. Mineral. Petrol. 123, 345–357.
Koornneef, J.M., Davies, G.R., Dopp, S.P., Vukmanovic, Z., Nikogosian, I.K., Mason, P.R.D., 2009. Nature and timing of multiple metasomatic events in the subcratonic lithosphere beneath Labait, Tanzania. Lithos 112, 896–912.
Kopylova, M., Matveev, S., Raudsepp, M., 2007. Searching for parental kimberlite melt. Geochim. Cosmochim. Acta 71, 3616–3629.
Lee, C., Rudnick, R., 1999. Compositionally stratified cratonic lithosphere: petrology and geochemistry of peridotite xenoliths from the Labait tuff cone, Tanzania. In: Proceedings of the 7th International Kimberlite Conference, pp. 503–521.
Lee, C.-T.A., Luffi, P., Chin, E.J., 2011. Building and destroying continental mantle. Annu. Rev. Earth Planet. Sci. 39, 59–90.
Lenardic, A., Moresi, L., 1999. Some thoughts on the stability of cratonic lithosphere – Effects of buoyancy and viscosity. J. Geophys. Res. 104, 12747–12759.
Lenardic, A., Moresi, L.-N., Mühlhaus, H., 2003. Longevity and stability of cratonic lithosphere: insights from numerical simulations of coupled mantle convection and continental tectonics. J. Geophys. Res. 108, 2303.
Li, Z.-X.A., Lee, C.-T.A., Peslier, A.H., Lenardic, A., Mackwell, S.J., 2008. Water contents in mantle xenoliths from the Colorado Plateau and vicinity: Implications for the mantle rheology and hydration-induced thinning of continental lithosphere. J. Geophys. Res. 113.
Maboko, M.A.H., 2000. Nd and Sr isotopic investigation of the Archean–Proterozoic boundary in north eastern Tanzania: constraints on the nature of Neoproterozoic tectonism in the Mozambique Belt. Precambrian Res. 102, 87–98.
Mackwell, S.J., Kohlstedt, D.L., 1990. Diffusion of hydrogen in olivine: implications for water in the mantle. J. Geophys. Res. 95, 5079–5088.
Manya, S., Kobayashi, K., Maboko, M.A.H., Nakamura, E., 2006. Ion microprobe zircon U–Pb dating of the late Archaean metavolcanics and associated granites of the Musoma–Mara Greenstone Belt, Northeast Tanzania: Implications for the geological evolution of the Tanzania Craton. J. Afr. Earth Sci. 45, 355–366.
McKenzie, D., Bickle, M., 1988. The volume and composition of melt generated by extension of the lithosphere. J. Petrol. 29, 625–679.
McLachlan, D., 1987. An equation for the conductivity of binary mixtures with anisotropic grain structures. J. Phys. C, Solid State Phys. 20, 865.
Mei, S., Kohlstedt, D., 2000. Influence of water on plastic deformation of olivine aggregates, 2. Dislocation creep regime. J. Geophys. Res., Solid Earth 105, 21471–21481.
Mierdel, K., Keppler, H., Smyth, J.R., Langenhorst, F., 2007. Water solubility in aluminous orthopyroxene and the origin of Earth's asthenosphere. Science 315, 364–368.
Möller, A., Appel, P., Mezger, K., Schenk, V., 1995. Evidence for a 2 Ga subduction zone – eclogites in the Usagaran Belt of Tanzania. Geology 23, 1067–1070.
Möller, A., Mezger, K., Schenk, V., 1998. Crustal age domains and the evolution of the continental crust in the Mozambique Belt of Tanzania: Combined Sm–Nd, Rb–Sr, and Pb–Pb isotopic evidence. J. Petrol. 39, 749–783.
Moser, D., Heaman, L., 1997. Proterozoic zircon growth in Archean lower crustal xenoliths, southern Superior craton – a consequence of Matachewan ocean opening. Contrib. Mineral. Petrol. 128, 164–175.
Moucha, R., Forte, A.M., 2011. Changes in African topography driven by mantle convection. Nat. Geosci. 4, 707–712.
Nyblade, A.A., 1997. Heat flow across the East African Plateau. Geophys. Res. Lett. 24, 2083–2086.
Nyblade, A.A., Pollack, H.N., Jones, D.L., Podmore, F., Mushayandebvu, M., 1990. Terrestrial heat-flow in east and southern Africa. J. Geophys. Res., Solid Earth Planets 95, 17371–17384.
O'Donnell, J., Adams, A., Nyblade, A., Mulibo, G., Tugume, F., 2013. The uppermost mantle shear wave velocity structure of eastern Africa from Rayleigh wave tomography: constraints on rift evolution. Geophys. J. Int. 194, 961–978.
O'Neill, C., Lenardic, A., Griffin, W., O'Reilly, S.Y., 2008. Dynamics of cratons in an evolving mantle. Lithos 102, 12–24.
O'Reilly, S.Y., Griffin, W., 2010. The continental lithosphere–asthenosphere boundary: Can we sample it?. Lithos 120, 1–13.
Paslick, C., Halliday, A., James, D., Dawson, J.B., 1995. Enrichment of the continental lithosphere by OIB melts – isotopic evidence from the volcanic province, Northern Tanzania. Earth Planet. Sci. Lett. 130, 109–126.
Peslier, A.H., 2010. A review of water contents of nominally anhydrous natural minerals in the mantles of Earth, Mars and the Moon. J. Volcanol. Geotherm. Res. 197, 239–258.
Peslier, A.H., Woodland, A.B., Bell, D.R., Lazarov, M., 2010. Olivine water contents in the continental lithosphere and the longevity of cratons. Nature 467, 78–81.
Petrick, W., Pelton, W., Ward, S., 1977. Ridge regression inversion applied to crustal resistivity sounding data from South Africa. Geophysics 42, 995–1005.
Phillips, D., Onstott, T., Harris, J., 1989. $^{40}Ar/^{39}Ar$ laser-probe dating of diamond inclusions from the Premier Kimberlite. Nature 340, 460–462.
Phillips, D., Machin, K., Kiviets, G., Fourie, L., Roberts, M., Skinner, E., 1998. A petrographic and 40 Ar/39 Ar geochronological study of the Voorspoed Kimberlite, South Africa: implications for the origin of Group II kimberlite magmatism. S. Afr. J. Geol. 101, 299–306.
Pik, R., Marty, B., Hilton, D., 2006. How many mantle plumes in Africa? The geochemical point of view. Chem. Geol. 226, 100–114.

Pollack, H.N., 1986. Cratonization and thermal evolution of the mantle. Earth Planet. Sci. Lett. 80, 175–182.
Prodehl, C., Ritter, J.R.R., Mechie, J., Keller, G.R., Khan, M.A., Jacob, B., Fuchs, K., Nyambok, I.O., Obel, J.D., Riaroh, D., 1997. The KRISP 94 lithospheric investigation of southern Kenya – the experiments and their main results. Tectonophysics 278, 121–147.
Reddy, S.M., Collins, A.S., Mruma, A., 2003. Complex high-strain deformation in the Usagaran Orogen, Tanzania: structural setting of Palaeoproterozoic eclogites. Tectonophysics 375, 101–123.
Reddy, S.M., Collins, A.S., Buchan, C., Mruma, A.H., 2004. Heterogeneous excess argon and Neoproterozoic heating in the Usagaran Orogen, Tanzania, revealed by single grain Ar-40/Ar-39 thermochronology. J. Afr. Earth Sci. 39, 165–176.
Ritsema, J., van Heijst, H., 2000. New seismic model of the upper mantle beneath Africa. Geology 28, 63–66.
Ritsema, J., Nyblade, A.A., Owens, T.J., Langston, C.A., VanDecar, J.C., 1998. Upper mantle seismic velocity structure beneath Tanzania, east Africa: Implications for the stability of cratonic lithosphere. J. Geophys. Res., Solid Earth 103, 21201–21213.
Roberts, E., Stevens, N., O'Connor, P., Dirks, P., Gottfried, M., Clyde, W., Armstrong, R., Kemp, A., Hemming, S., 2012. Initiation of the western branch of the East African Rift coeval with the eastern branch. Nat. Geosci. 5, 289–294.
Rooney, T.O., Herzberg, C., Bastow, I.D., 2012. Elevated mantle temperature beneath East Africa. Geology 40, 27–30.
Rudnick, R., McDonough, W.F., Orpin, A., 1994. Northern Tanzanian peridotite xenoliths: A comparison with Kaapvaal peridotites and interences on metasomatic interactions. In: Meyer, H.O.A., Leonardos, O.H. (Eds.), Fifth International Kimberlite Conference. Brasilia, pp. 336–353.
Seggie, A., Hannweg, G., Colgan, E., Smith, C., 1999. The geology and geochemistry of the Venetia kimberlite cluster, Northern Province, South Africa. In: Proceedings of the 7th International Kimberlite Conference. Cape Town, South Africa, pp. 750–756.
Selway, K., 2013. On the causes of electrical conductivity anomalies in tectonically stable lithosphere. Surv. Geophys., 1–39.
Selway, K., Hand, M., Heinson, G.S., Payne, J.L., 2009. Magnetotelluric constraints on subduction polarity: Reversing reconstruction models for Proterozoic Australia. Geology 37, 799–802.
Skemer, P., Karato, S.-i., 2008. Sheared lherzolite xenoliths revisited. J. Geophys. Res. 113, B07205.
Sleep, N.H., Ebinger, C.J., Kendall, J.M., 2002. Deflection of mantle plume material by cratonic keels. In: Early Earth: Physical, Chemical and Biological Development. Geol. Soc. (Lond.) Spec. Publ. 199, 135–150.
Smith, C.B., Clark, T.C., Barton, E.S., Bristow, J.W., 1994. Emplacement ages of kimberlite occurrences in the Prieska region, southwest border of the Kaapvaal Craton, South Africa. Chem. Geol. 113, 149–169.
Smithies, R., Van Kranendonk, M., Champion, D., 2005. It started with a plume – early Archaean basaltic proto-continental crust. Earth Planet. Sci. Lett. 238, 284–297.
Sommer, H., Kroner, A., Hauzenberger, C., Muhongo, S., 2005. Reworking of Archaean and Palaeoproterozoic crust in the Mozambique belt of central Tanzania as documented by SHRIMP zircon geochronology. J. Afr. Earth Sci. 43, 447–463.
Stachel, T., Harris, J.W., Brey, G.P., 1998. Rare and unusual mineral inclusions in diamonds from Mwadui, Tanzania. Contrib. Mineral. Petrol. 132, 34–47.
Stern, R.J., 1994. Arc-assembly and continental collision in the Neoproterozoic African Orogen: Implications for the consolidation of Gondwanaland. Annu. Rev. Earth Planet. Sci. 22, 319–351.
Stripp, G., Field, M., Schumacher, J., Sparks, R., Cressey, G., 2006. Post-emplacement serpentinization and related hydrothermal metamorphism in a kimberlite from Venetia, South Africa. J. Metamorph. Geol. 24, 515–534.
Tenczer, V., Fritz, H., Bauernhofer, A., Hauzenberger, C., 2007. Two orogens – one shear belt: 1 Ga of repeated deformation along the Central Tanzanian Shear Belt. J. Struct. Geol. 29, 1632–1649.
Thiel, S., 2008. Modelling and Inversion of Magnetotelluric Data for 2D and 3D Lithospheric Structure, with Application to Obducted and Subducted Terranes. University of Adelaide, Adelaide.
Turcotte, D.L., Schubert, G., 2002. Geodynamics. Cambridge University Press.
Vauchez, A., Dineur, F., Rudnick, R., 2005. Microstructure, texture and seismic anisotropy of the lithospheric mantle above a mantle plume: Insights from the Labait volcano xenoliths (Tanzania). Earth Planet. Sci. Lett. 232, 295–314.
Venkataraman, A., Nyblade, A.A., Ritsema, J., 2004. Upper mantle Q and thermal structure beneath Tanzania, East Africa from teleseismic P wave spectra. Geophys. Res. Lett. 31, L15611.
Ward, S.H., Hohmann, G.W., 1988. Electromagnetic theory for geophysical applications. In: Electromagnetic Methods in Applied Geophysics, vol. 1, pp. 131–311.
Weeraratne, D.S., Forsyth, D.W., Fischer, K.M., Nyblade, A.A., 2003. Evidence for an upper mantle plume beneath the Tanzanian craton from Rayleigh wave tomography. J. Geophys. Res., Solid Earth 108.
Workman, R.K., Hauri, E., Hart, S.R., Wang, J., Blusztajn, J., 2006. Volatile and trace elements in basaltic glasses from Samoa: Implications for water distribution in the mantle. Earth Planet. Sci. Lett. 241, 932–951.
Wyman, D.A., Kerrich, R., 2002. Formation of Archean continental lithospheric roots: the role of mantle plumes. Geology 30, 543–546.
Yoshino, T., Matsuzaki, T., Shatskiy, A., Katsura, T., 2009. The effect of water on the electrical conductivity of olivine aggregates and its implications for the electrical structure of the upper mantle. Earth Planet. Sci. Lett. 288, 291–300.